NJC

New Journal of Chemistry

An international journal of the chemical sciences

www.rsc.org/njc

Volume 32 | Number 10 | October 2008 | Pages 1645–1808

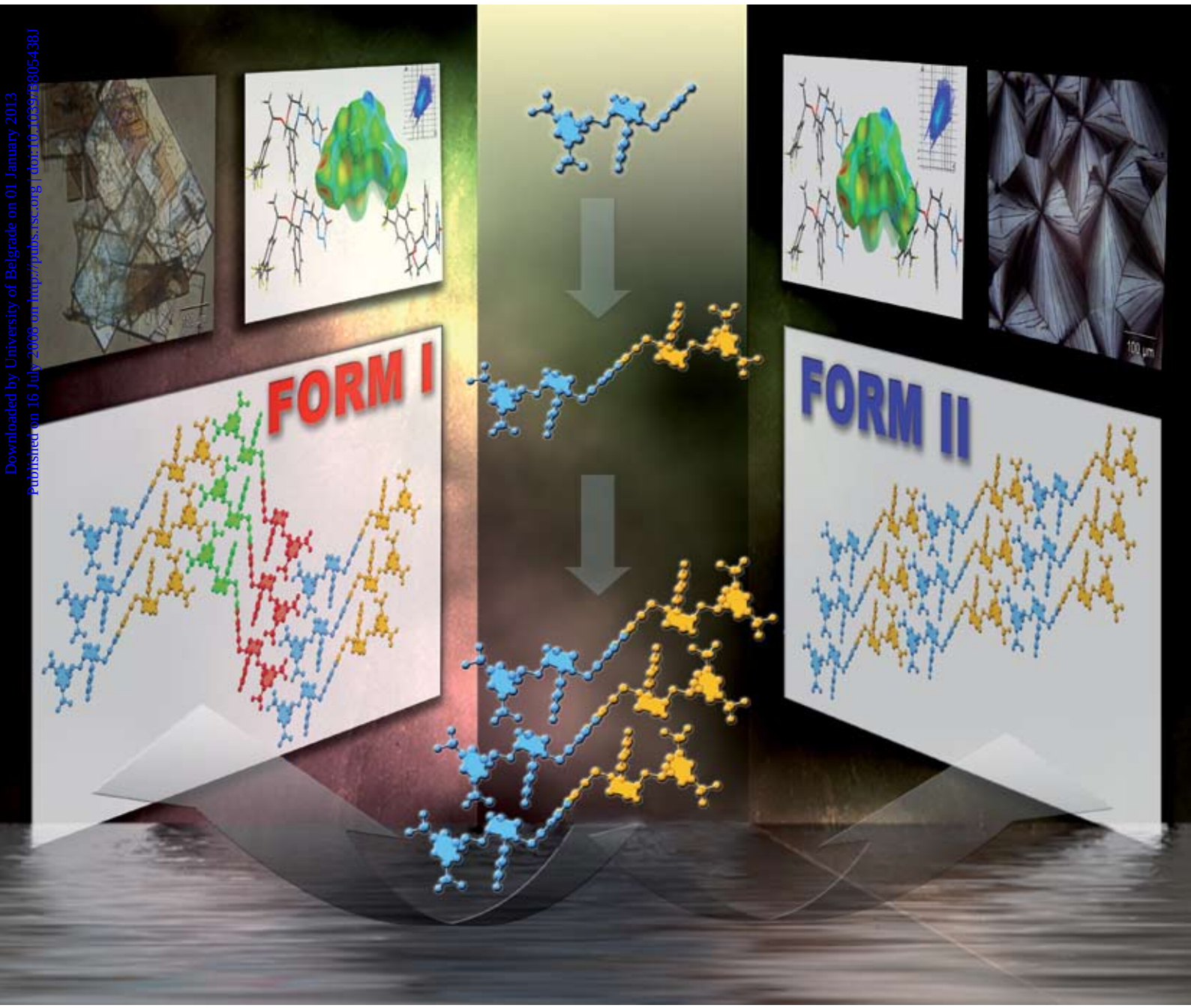

ISSN 1144-0546

RSC Publishing

CNRS CENTRE NATIONAL DE LA RECHERCHE SCIENTIFIQUE

THEMED ISSUE
Polymorphism and crystal forms

Packing polymorphism of a conformationally flexible molecule (aprepitant)†

Doris E. Braun,[a] Thomas Gelbrich,[a] Volker Kahlenberg,[b] Gerhard Laus,[c] Josef Wieser[d] and Ulrich J. Griesser*[a]

Received (in Montpellier, France) 3rd April 2008, Accepted 8th May 2008
First published as an Advance Article on the web 16th July 2008
DOI: 10.1039/b805438j

This work highlights the structural and thermochemical differences of two modifications of the NK_1 receptor antagonist aprepitant. Form I° is the stable polymorph and crystallises in the orthorhombic space group $P2_12_12_1$ whereas the metastable form II is monoclinic (space group $P2_1$). The monotropically related polymorphs show only minor differences in melting point and heat of fusion ($T_{fus,I}$ = 253.6, $\Delta_{fus}H_I$ = 53.7 kJ mol^{-1}, $T_{fus,II}$ = 253.0 °C, $\Delta_{fus}H_{II}$ = 52.4 kJ mol^{-1}) and often crystallise concomitantly. The forms exhibit a very close structural relationship based on a common 2D packing fragment, which is in fact a stack of 1D N–H···O hydrogen bonded ribbon chains. Forms I° and II may therefore be interpreted as two distinct stacking modes of this common 2D unit. The alternative modes are associated with slight differences in weaker intermolecular interactions. Somewhat surprisingly, the aprepitant molecule adopts almost the same conformation in the two crystal structures in spite of its potential conformational flexibility. Hirshfeld surface analysis was successfully deployed to visualise and elaborate the small differences in the molecular environments of the two polymorphs. The study emphasises the benefit of single-crystal structure data for the judgement of the phase purity and of polymorphs exhibiting only weak energetical and structural differences.

Introduction

Aprepitant (5-{2-[1-(3,5-bis(trifluoromethyl)phenyl)ethoxy]-3-(4-fluorophenyl)morpholin-4-ylmethyl}-2,4-dihydro-1,2,4-triazol-3-one, Emend®, Fig. 1) is the first commercially available neurokinin 1 (NK_1) receptor antagonist. NK_1 receptor antagonists are being investigated for the treatment of depression, migraine, pain, and emesis. The substance is administered orally in combination with other agents, and mainly indicated for the prevention of acute and delayed chemotherapy-induced nausea and vomiting associated with highly emetogenic chemotherapy in adults.[1]

The importance of identifying and characterising different crystal forms of a drug has been well documented in the literature.[2] Differences in solubility, dissolution rate, morphology, mechanical properties, and physicochemical stability of different crystal forms demand a detailed study of polymorphism of any new drug molecule.[3] Patenting new solid state forms is an important part of modern life-cycle management of innovative pharmaceutical compounds.[4]

The synthesis of aprepitant has been disclosed in example 75 of the patent WO 95/16679.[5] In a subsequent patent, WO 99/01444,[6] it was mentioned that this compound crystallised initially as form II, and this document describes the new form I°, as well as form II, in more detail. However, only the room-temperature structure of one polymorph (form I°, the superscript zero marks the thermodynamically stable form at 20 °C) has been reported so far (CSD refcode: GOPDUK[7]). It was found to crystallise in the non-centrosymmetric space group $P2_12_12_1$ with four molecules in the unit cell (Z' = 1), but neither the geometrical features of the aprepitant molecules, nor their packing in the crystal structure were discussed in that report. In addition to the two polymorphs, the amorphous state was disclosed in a patent application,[8] while another such

[a] *Institute of Pharmacy, University of Innsbruck, Innrain 52, 6020 Innsbruck, Austria*
[b] *Institute of Mineralogy and Petrography, University of Innsbruck, Innrain 52, 6020 Innsbruck, Austria*
[c] *Institute of General, Inorganic and Theoretical Chemistry, University of Innsbruck, Innrain 52a, 6020 Innsbruck, Austria*
[d] *Sandoz GmbH, Biochemiestrasse 10, 6250 Kundl, Austria. E-mail: Ulrich.Griesser@uibk.ac.at; Fax: 0043 512 507 2939; Tel: 0043 512 5309*

† Electronic supplementary information (ESI) available: Light photomicrographs, thermal ellipsoid plots, 1D ribbon formed by the strong hydrogen bonds, different Hirshfeld surface plots (d_e, fingerprint, and shape index) for the two aprepitant polymorphs and energy/temperature diagram. CCDC reference numbers 687301 (form I°) and 687301 (form II). For ESI and crystallographic data in CIF or other electronic format see DOI: 10.1039/b805438j

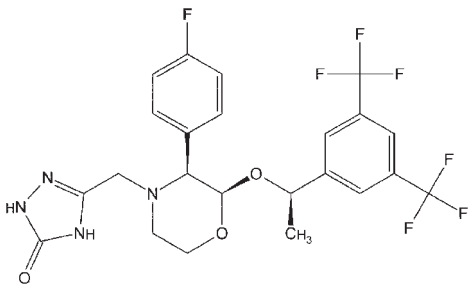

Fig. 1 Molecular structure of aprepitant.

application[9] describes mixtures composed of the two polymorphs.

The two polymorphic forms show only minor spectral and thermochemical differences.[6,10] The aim of our investigation was therefore to determine how their structures relate to one another and whether relationships can be identified that would explain such a behaviour. We succeeded in obtaining crystals suitable for a single-crystal structure analysis and expected that the examination of strong and weak intermolecular interactions and a XPac[11] comparison of the crystal packing modes would lead us to a deeper understanding of this polymorphic system. A Hirshfeld surface analysis[12] was performed to visualise and discriminate the features of the molecular interactions in the two structures.

Experimental

General comments

Aprepitant (purity 99.0%) was prepared by a combination of published procedures.[13] The obtained product consisted of a mixture of form I° and form II. The solvents used in this study were of analytical grade.

Preparation of the single crystals

Crystals of form I° which proved to be suitable for a single-crystal X-ray structure analysis were obtained by crystallisation (heat/cool) of aprepitant from several solvents such as acetonitrile, DMSO, acetic acid, ethyl acetate, DMF, 1-PrOH, EtOH, a mixture of DMSO–water or THF–water. Form II single crystals were obtained *via* crystallisation from an acetone–water mixture.

Single-crystal X-ray diffractometry

The X-ray data were collected at −100 °C on a STOE IPDS-II diffractometer using Mo-Kα radiation (λ = 0.71073 Å). The structure solution and refinement were carried out using the SIR97 and SHELXL97 programs incorporated in the WinGX program suit.[14] All hydrogen atoms bound to carbon atoms were generated by a riding model in idealised geometries and their positions refined with $U_{iso}(H) = 1.5\ U_{eq}(C)$ for $-CH_3$ groups and $U_{iso}(H) = 1.2\ U_{eq}(C)$ for all other hydrogen atoms. The amide hydrogen atoms in form I° were located from difference Fourier maps and refined without any constraints, whereas in form II they were generated by a riding model in idealised geometries and refined with $U_{iso}(H) = 1.2\ U_{eq}(N)$. The fluorine atoms in one of the $-CF_3$ groups of form I° were found to be statistically disordered over two positions with an occupancy of 0.60 : 0.40. The anisotropic displacement parameters of the six disordered $-CF_3$ fluorine atoms attached to C(23) were restrained to being approximately isotropic, using the ISOR command in SHELXL with a standard uncertainty of 0.008. Despite our best efforts, only very small single crystals of inferior quality could be obtained for form II. Observation of these crystals under a polarising microscope with crossed polarisers showed no clear extinction position and pointed to the presence of non-merohedral twinning. The single-crystal diffraction experiments confirmed this hypothesis: the diffraction pattern could be explained by a superposition of two reciprocal lattices related by a rotation of 180° about b^*. The Stoe X-AREA[15] software package was employed to isolate the diffraction spots originating from the two distinct domains. The diffraction peaks were indexed independently and the two superimposed patterns were integrated simultaneously including an overlap check. For structure solution only the non-overlapping reflections were used. For the subsequent refinement the completely overlapping reflections were considered as well (HKLF5 data format of SHELXL-97). The anisotropic displacement parameters of the $-CF_3$ fluorine atoms in form II were restrained to being approximately isotropic, using the ISOR command in SHELXL with a standard uncertainty of 0.008. The chemically equivalent C–C bond lengths in the bistrifluoromethyl substituted phenyl ring and the chemically equivalent O1–C2 and O1–C3 bond distances in the morpholine ring were restrained using the SHELXL SADI command with a standard uncertainty of 0.01. From X-ray analysis only the relative, and not the absolute stereochemistries of the two forms could be determined.

CCDC reference numbers 687301 (form I°) and 687301 (form II).

For crystallographic data in CIF or other electronic format see DOI: 10.1039/b805438j

Powder X-ray diffractometry

The X-ray diffraction patterns (PXRD) were obtained with a Siemens D-5000 diffractometer (Siemens AG, Karlsruhe, Germany) equipped with a theta/theta goniometer, a CuKα radiation source, a Goebel mirror (Bruker AXS, Karlsruhe, Germany), a 0.15° Soller slit collimator, and a scintillation counter. The patterns were recorded at a tube voltage of 40 kV and a tube current of 35 mA, applying a scan rate of 0.005° $2\theta\ s^{-1}$ in the angular range of 2–40° 2θ.

Differential scanning calorimetry

Differential scanning calorimetry (DSC) was performed with a DSC 7 (Perkin-Elmer, Norwalk, CT, USA) using the Pyris 2.0 software. Approximately 1 ± 0.0005 mg sample (using a UM3 ultramicrobalance, Mettler, Greifensee, CH) was weighed into Al-pans (25 µl). Dry nitrogen was used as the purge gas (purge: 20 ml min^{-1}). Heating rates of 10 K min^{-1} were routinely used. The instrument was calibrated for temperature with pure benzophenone (mp 48.0 °C) and caffeine (mp 236.2 °C) and the energy calibration was performed with pure indium (purity 99.999%, mp 156.6 °C, $\Delta_{fus}H$: 28.45 J g^{-1}). The errors of the stated temperature and enthalpy values are calculated as 95% confidence intervals (c.i.) based on at least five measurements.

Results and discussion

The structure determination carried out on a low-temperature data set confirms a previously reported crystal structure analysis of form I°,[7] but the R values and other indicators show that this redetermination is a substantial improvement. Furthermore, we were also able to determine the single-crystal structure of the second polymorph, form II, which crystallises in the non-centrosymmetric monoclinic space group $P2_1$ with one independent molecule in the asymmetric unit (Z = 2).

Table 1 Crystallographic data for aprepitant polymorphs

	I°	II
Chemical formula	$C_{23}H_{21}F_7N_4O_3$	$C_{23}H_{21}F_7N_4O_3$
M_r	534.44	534.44
Description	Colorless plates	Colorless thin plates
Size/mm	0.4 × 0.4 × 0.12	0.4 × 0.4 × 0.03
Melting point/°C	253.6	253
Crystal system	Orthorhombic	Monoclinic
Space group	$P2_12_12_1$	$P2_1$
T/K	173(2)	173(2)
a/Å	7.421(4)	7.7768(16)
b/Å	7.710(4)	7.4072(11)
c/Å	42.200(2)	21.297(5)
β/°	90.00	92.861(17)
V/Å^3	2414.5(18)	1225.2(4)
Z/Z'	4/1	2/1
D_c/Mg m^{-3}	1.470	1.449
Reflns. collected	17 601	6918
Independent reflns.	2894	6918
Observed reflns.	2536	5441
θ range for data collection/°	1.93–26.79	1.91–24.99
Range h	−9 to 9	−8 to 8
Range k	−8 to 9	−8 to 8
Range l	−53 to 53	−25 to 24
Data, restraints, parameters	2894, 42, 372	3294, 152, 336
Goodness of fit on F^2	1.18	1.06
R_{int}	0.0322	— (Twin)[a]
Final R indices [$I > 2\sigma(I)$]	R_1 = 0.0482, wR_2 = 0.1325	R_1 = 0.0903, wR_2 = 0.1775
R indices (all data)	R_1 = 0.0532, wR_2 = 0.1389	R_1 = 0.1165, wR_2 = 0.1910
$\Delta\rho_{max}$, $\Delta\rho_{min}$/e Å^{-3}	0.21, −0.2	0.36, −0.40

[a] Twin refinement. No R_{int} given due to automatic switch off of MERG in SHELXL HKLF5 mode.

Crystallographic data of the aprepitant polymorphs are given in Table 1.

Molecular geometry

The overlay of the molecules (Fig. 2) and the selection of torsion angles in Table 2 suggest that the molecules adopt virtually the same conformation in the two modifications. The variation in the torsion angles is negligible. Thus, the structures must differ in the packing arrangement, but the nature of the differences in their packing environments must be such that the same molecular geometry can be adopted in each case. This conclusion is somewhat surprising in view of the potential molecular flexibility of this molecule. We thus may regard this case as a prominent example of *packing polymorphism*[16] of a conformationally flexible molecule.

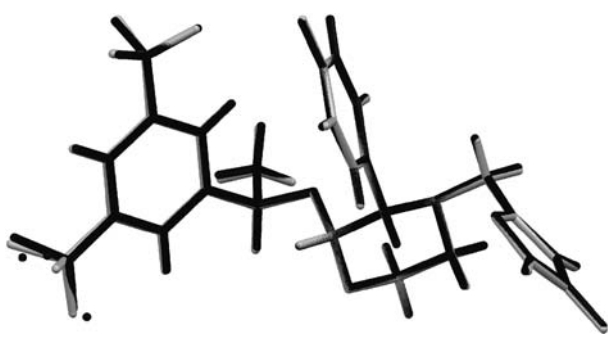

Fig. 2 Overlay of the aprepitant molecules in form I° (black) and II (grey).

Discussion of crystal structures and packing relationships

The triazolone moiety of the aprepitant molecule contains two N–H groups and one carbonyl oxygen atom which act as donor and two-fold acceptor sites, respectively, for H-bonds. The cyclic urea function of the triazolone ring is constrained in a *cis* arrangement so that both the hydrogen-bond donor and acceptor functions point in the same direction. Two independent N–H···O hydrogen bonds are formed in a single $R_2^2(8)$ ring.[17] This H-bonded arrangement is present in each modification and leads to the one-dimensional ribbon chain shown in Fig. 3 which exhibits 2_1 symmetry and propagates along the *a* axis in form I° and along the *b* axis in form II. The N–H···O distances and N–H···O angles (Table 3) agree well with the values tabulated by Gartland and Craven[18] and are typical for intermolecular interactions in derivatives of urea. A search of the Cambridge Structural Database (CSD)[19] for chemically similar fragments (strong H-bonded molecular ribbons with urea as functional group) resulted in 43 hits, confirming that this is a preferred mode of aggregation.

Table 2 Conformational data for aprepitant polymorphs

Form	I°	II
N(1)–C(5)–C(6)–N(2)	89.4(3)	88.3(8)
N(1)–C(5)–C(6)–N(4)	−88.9(3)	−85.3(9)
N(1)–C(1)–C(8)–C(9)	−135.1(3)	−134.0(6)
N(1)–C(1)–C(8)–C(13)	48.2(4)	48.1(8)
C(2)–O(3)–C(14)–C(15)	81.3(3)	83.0(7)
O(3)–C(14)–C(15)–C(16)	55.4(4)	53.7(8)
O(3)–C(14)–C(15)–C(20)	−127.3(3)	−129.5(6)

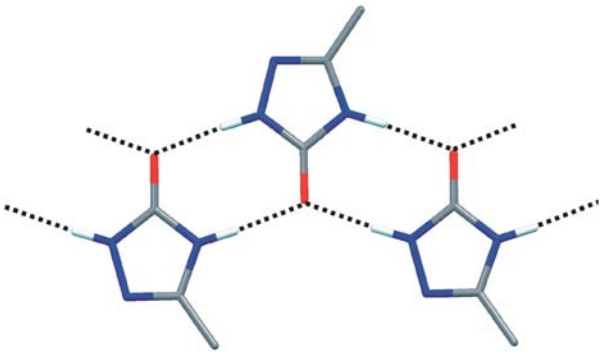

Fig. 3 N–H···O hydrogen bonds of the aprepitant polymorphs forming a 1D ribbon chain.

The XPac program[11] was used to establish the relationship between forms I° and II with regard to their molecular packing. It was found that the two modifications not only share the same connectivity of their N–H···O interactions, but that the H-bonded chains resulting from these interactions also have virtually the same geometry in each case. Additionally, these chains are stacked in the same fashion in the two forms. Thus, I° and II are very closely related, exhibit a 2D packing similarity, and may be interpreted as two alternative packing modes of the same stack of N–H···O bonded chains of aprepitant molecules or, alternatively, of different stacking modes of a common double sheet of molecules.

This relationship is further explored in Fig. 4. It shows an *Aufbau*[20] of the two polymorphs, starting with the aprepitant molecule, which leads *via* the H-bonded chains and the stack of chains, which is the common 2D fragment of forms I° and II. The N–H···O bonded chains exhibit 2_1 symmetry, and additional 2_1 axes lie between neighbouring chains in this stack generated by translation symmetry. The resulting common 2D structure fragment (or supramolecular construct[11]) of I° and II lies parallel to an *ab*-plane in each modification. However, the *a*-axis of form I° corresponds to the *b*-axis of form II (this is the direction of H-bonded chains). Furthermore, adjacent chains, related by translation symmetry form a stack which propagates along the *b*-axis in form I° and along the *a*-axis in modification II. The very close agreement within the two pairs of corresponding lattice parameters associated with the translation in the H-bonded chain (7.42/7.40 Å) and the stack of chains (7.71 Å/7.78 Å) is a direct result of this packing relationship.

However, forms I° and II differ in the way in which this common 2D unit is linked to its two neighbouring units along the respective *c*-axis. The stacking of adjacent units by translation results in the $P2_1$ structure of form II. It can be seen from Fig. 4 that this process generates an additional set of 2_1 axes at the contact surfaces of two such units, which lies parallel to the first set, and the resulting space group symmetry is $P2_1$. By contrast, a stacking mode where the neighbouring common 2D units are related by 2_1 symmetry operations perpendicular to those of the H-bonded chains also generates a third set of 2_1-axes which is perpendicular to each of the former two. This results in the $P2_12_12_1$ structure of modification I°. Thus, both the length of the *c*-axis and the size of the unit cell of form I° are doubled with respect to form II. Fig. 5 shows a more detailed view of the different packing arrangements in the two polymorphs. The same projection is used as for Fig. 4.

The identified packing relationship means that the spatial arrangement in a cluster composed of a central aprepitant molecule and 11 of its 14 closest neighbours is almost exactly the same in the two forms. Thus, almost 80% of a molecule's environment is maintained, which also explains why the same geometry of the aprepitant molecule is observed each time—this is the consequence of the close 2D packing similarity. Furthermore, the effect of the environment defined by the remaining three neighbours must be approximately equally favourable in the two forms to make their packing modes feasible. The striking similarity observed in the physical properties of forms I° and II can therefore be interpreted as a consequence of the preservation of almost all nearest neighbour interactions in conjunction with that of the molecular geometry.

The presence of two or more alternative stacking modes of a common 2D structure fragment is probably the most important

Table 3 Geometrical parameters for the hydrogen bonds and weak intermolecular interactions[ab] for aprepitant polymorphs. Interactions within the common 2D structure fragment of forms I° and II are indicated by an asterisk. Distances are given in Å and angles in °.

Form		Interaction	H···A	D···A	D–H–A
Form I°	*	N(2)–H···O(2)[e]	1.83	2.834(4)	175
	*	N(3)–H···O(2)[f]	1.81	2.817(4)	175
	*	C(3)–H···F(7)[g]	2.43	3.090(5)	118
	*	C(4)–H···F(7)[g]	2.40	2.901(4)	107
		C(18)–H···F(4)[h]	2.34	3.426(13)	177
		C(18)–H···F(4A)[h]	2.48	3.531(13)	163
	*	C(5)–H···N(4)[i]	2.56	3.367(4)	130
	*	C(12)–H···π	2.89[c]/2.87[d]	3.473(4)	121
Form II	*	N(2)–H···O(2)[j]	1.84	2.837(7)	171
	*	N(3)–H···O(2)[k]	1.80	2.808(7)	175
	*	C(3)–H···F(7)[l]	2.44	3.102(10)	118
	*	C(4)–H···F(7)[l]	2.40	2.902(9)	106
	*	C(5)–H···N(4)[m]	2.63	3.405(9)	128
	*	C(12)–H···π	2.96[c]/2.94[d]	3.521(8)	119

[a] The sum of the van der Waals radii was used as cut-off parameter. [b] All N–H, and C–H distances were neutron normalised to 1.009, and 1.083 Å using the program PLATON.[27] [c] Centroid distances. [d] Perpendicular distances. Symmetry code: [e] $x + 1/2, -y + 1/2, -z$. [f] $x - 1/2, -y + 1/2, -z$. [g] $x - 1, +y - 1, +z$. [h] $-x + 2, +y - 1/2, -z + 1/2$. [i] $x - 1/2, -y + 3/2, -z$. [j] $-x + 2, +y + 1/2, -z + 1$. [k] $-x + 2, +y - 1/2, -z + 1$. [l] $x + 1, +y + 1, +z$. [m] $-x + 1, +y + 1/2, -z + 1$.

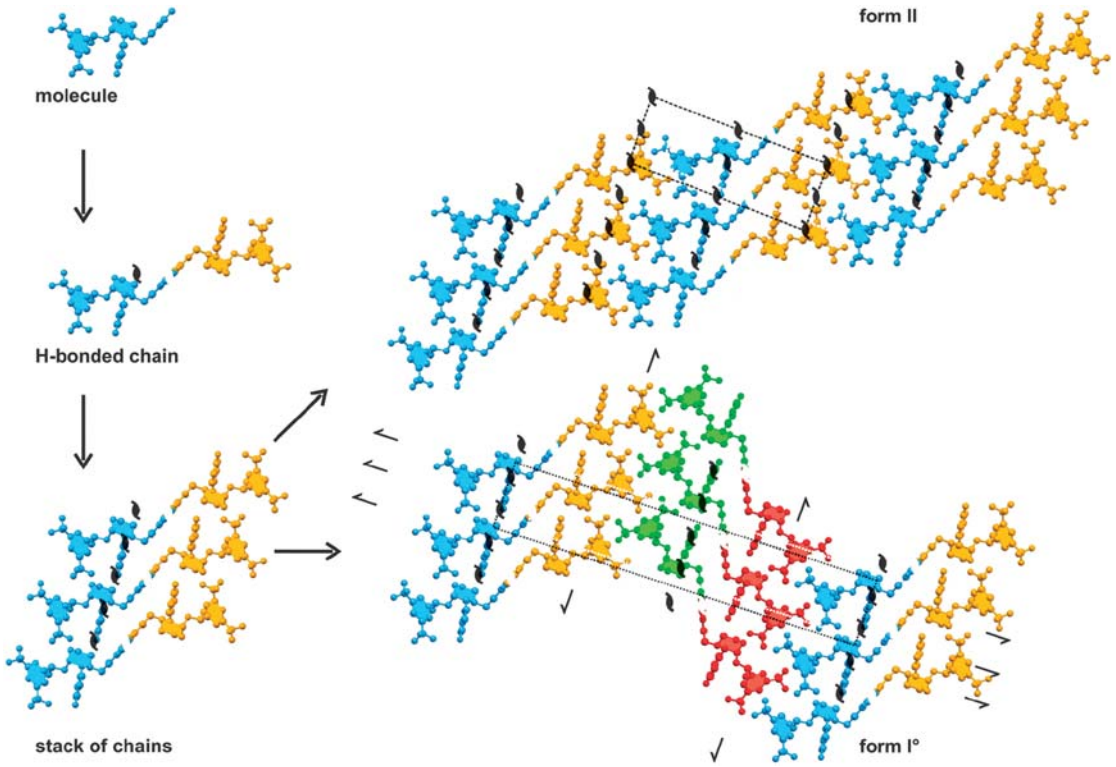

Fig. 4 A formal *Aufbau* of forms I° and II of aprepitant. The structures are viewed along the respective translation vector of the N–H···O bonded chains. Left from top: (a) Single aprepitant molecule (blue). (b) 1D N–H···O bonded ribbon chain composed of two sets of molecules related by 2_1 symmetry (blue/yellow). (c) Stack of ribbon chains generated by translation symmetry and an additional set of 2_1 axes parallel to the first set (this is the common 2D fragment of forms I° and II). Right top: Structure of form II, viewed along the *b*-axis. Neighbouring stacks of chains are related by translation symmetry, so that additional 2_1 axes parallel to those in each stack of chains are generated. Right bottom: Structure of form I°, viewed along the *a*-axis. Neighbouring stacks of chains are related by two sets of 2_1 axes, each lying perpendicular to the 2_1 axes of the stack of chains. This generates a second orientation for these 2D units (green/red).

kind of packing polymorphism which can be observed in molecular crystal structures. Examples include the drugs aspirin[21] and sulfathiazole (three of its forms are related in this way),[22] the explosive TNT,[23] and a group of compounds prepared as non-linear optical materials.[24] The occurrence of 2D packing polymorphism is not restricted to those molecules which are rather small and rigid, but there are also examples involving more complex molecular geometries (see first case study in ref. 11). Timofeeva *et al*. have used the term "organic polytypism",[24] in order to emphasise the analogy to the polytypism observed in inorganic structures (but there are no organic structure types), and the terms "partial isostructurality"[25a] and "two-dimensional isostructurality"[25b,c] have also been used. The molecular geometry is typically maintained, and the common structure fragment can be a single sheet, a double layer or an even thicker layer of molecules. One consequence of 2D packing similarity is that two translation vectors and their angle of intersection are equivalent in the polymorphs involved, which is usually visible in the unit cell constants of *P*-type structures. Another consequence is the possible occurrence of stacking faults, and the presence of two competing modes of connecting 2D sheets is a prescription for the formation of twins, and the intergrowth of such phases has been recently described for aspirin.[21b] The problems experienced in this study with regard to the twinning of form II have probably the same background.

A number of weak, non-standard interactions of the C–H···F type[26] can be identified in forms I° and II. The first of these involves the fluorine atom F(7) of the fluorophenyl ring, which interacts with two hydrogen atoms of the morpholine ring. This contact is associated with the 1D stacking of N–H···O bonded chains in the common 2D structure fragment, and it is therefore observed in both forms.

By contrast, additional weak interactions of the C–H···F type are found only in form I°. They involve molecules originating from neighbouring stacks of chains which are related by a 2_1 screw axis along *c* and are therefore intrinsically linked with the specific packing in form I°. One of the fluorine atoms of the disordered trifluoromethyl group (the two hypothetical torsional positions are in the proximity to form this weak interaction) and an ortho positioned hydrogen atom of the same ring in one neighbouring molecule are engaged in this interaction. The distance of this interaction is longer than that involving the F(7) atom, but the C–H···F angle is closer to 180°. Geometrical parameters for all strong and weak interactions are listed in Table 3. The parameters associated with interactions within the common 2D structure fragment of forms I° and form II (indicated by an asterisk) show a striking preservation of geometry and provide further evidence for the discussed relationship between the two modifications.

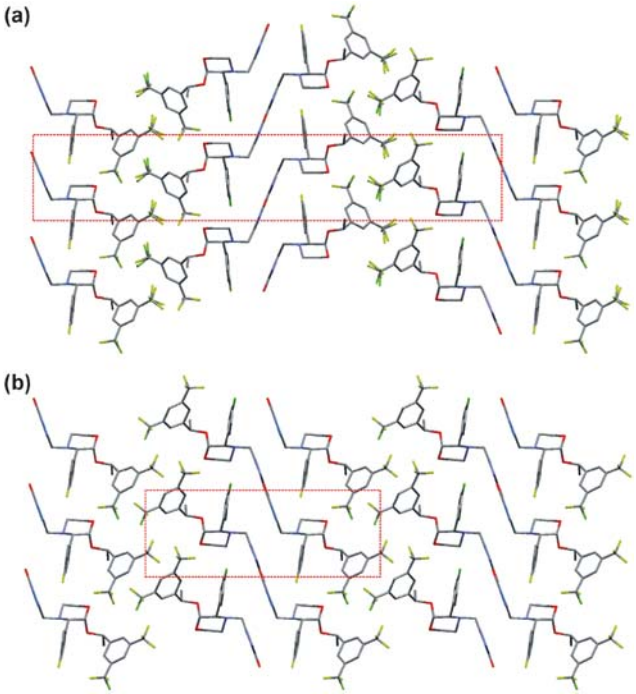

Fig. 5 Packing views and schematic packing illustration of the two aprepitant forms I° (a) and II (b). Form I° is viewed along the *a* axis, form II along the *b* axis. The unit cells are highlighted as dotted lines.

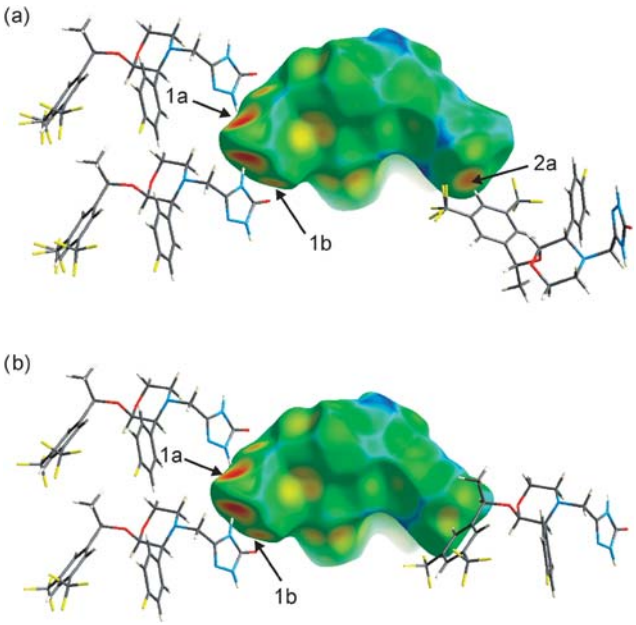

Fig. 6 Hirshfeld surfaces of aprepitant polymorphs (a) form I° and (b) form II. d_e Surfaces have been mapped between d_e 0.73 and 2.7 Å. 1a marks the acceptor, 1b the donor of the stronger (shorter) of the two N–H···O hydrogen bonds. The label 2a marks the fluorine atom (acceptor, F(4)/F(4A)) of the C–H···F interaction only present in form I°.

Hirshfeld surface analysis

Hirshfeld surfaces are constructed by partitioning the space in a crystal into regions where the electron density from the sum of spherical atoms of the molecule is greater than the corresponding sum over the crystal.[12] Many applications in the recent past demonstrated that this analysis can be very valuable in the exploration of the packing modes and intermolecular interactions in molecular crystals.[28] Since the two polymorphs of aprepitant show no substantial conformational differences the Hirshfeld surface analysis seemed to be particularly promising for the visualisation of variations in the environments of the molecules. We used the program Crystal Explorer[29] for this task.

The Hirshfeld surfaces for the two aprepitant polymorphs are illustrated in Fig. 6, showing surfaces that have been mapped over the d_e range 0.73–2.7 Å. A mapping from red, for short d_e ranges, to blue, long ranges, was employed. The two forms of aprepitant show similar intermolecular interactions. The surfaces display the two strong hydrogen bonds (N–H···O) as well as the weak (C–F···H) and (C–F···π) interactions, and H···H short contacts. Red spots on the d_e surface indicate the hydrogen bonds. In any H-bond a large red region appears adjacent to the H-bond acceptor, while a smaller orange spot marks the H-bond donor. The two strong N–H···O hydrogen bonds which form the same type of interaction in the two modifications can be clearly recognised at the Hirshfeld surfaces (left side in Fig. 6, similar arrangement of the neighbour molecules in the two polymorphs). The presence of the additional weak interaction of the C–H···F type (F(4) and F(4A) of the $–CF_3$ group) in form I° appears as an orange-red dot (acceptor, marked with an arrow labelled as 2a in Fig. 6) and is the most striking difference between the Hirshfeld surfaces (d_e) of the two polymorphs. The different packing of the molecule in the environment of this CF_3 group is apparent in Fig. 6.

The 2D fingerprint plots[12,30] are given in Fig. 7. The fact that hardly any difference between the two polymorphs can be derived from their 2D fingerprint plots indicates that intermolecular interactions in the two modifications must be very similar. This is consistent with our previous assessments with regard to the close 2D packing similarity of forms I° and II, which means that roughly 80% of nearest-neighbour contacts in these modifications are almost identical. The two long spikes in each plot (marked with 1 in Fig. 7) represent the strong N–H···O hydrogen bonds in the common 2D structure fragment. As only the shortest C–H···F interaction occurs as a spike in the plot (labels 2a and 2b in Fig. 7), the longer C–H···F interaction, which is a characteristic only of form I° (involving the F(4) and F(4a) atoms of the disordered $–CF_3$ group), does not show up in the 2D plot if the two possible positions of the disordered group are modelled together and overlayed in one plot. The broadening of the spikes arises from the angles deviating from 180°. The C–H···F interactions occur around d_e = 1.1 Å – d_i = 1.3 Å and d_e = 1.3 Å – d_i = 1.1 Å. Further Hirshfeld plots (d_e and fingerprint plots), where the disordered form I was separated into two hypothetical "ordered" structures are given in ESI† (Fig. S5 and S6). Another kind of interaction within the common 2D structure fragment of I° and II are C–H···π contacts involving the triazolone ring as an acceptor. These give rise to characteristic wings in the region of d_e = 1.2 Å–d_i = 1.9 Å and d_e = 1.9 Å–d_i = 1.2 Å (marked with 3a and 3b in Fig. 7) in the

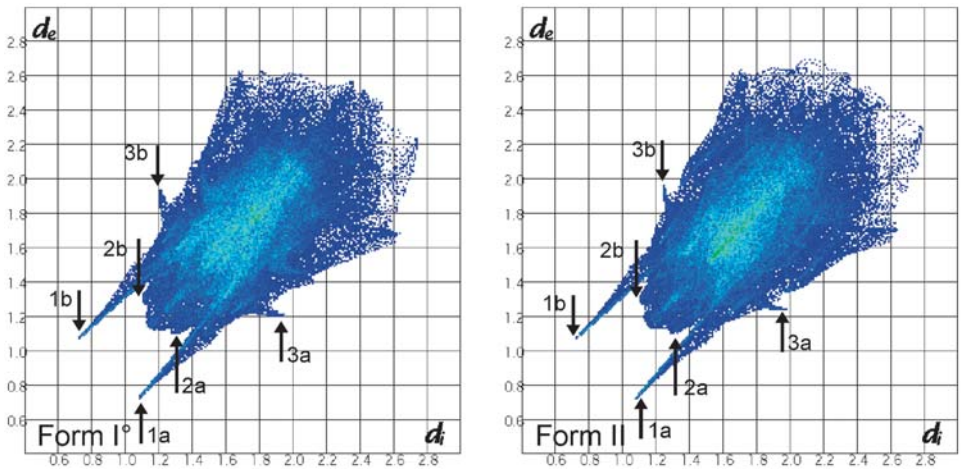

Fig. 7 2D fingerprint plots for form I° (left) and form II (right) of aprepitant; d_e and d_i are the distances to the nearest atom centre exterior and interior to the surface.

corresponding fingerprint plots. A slight difference occurs in the upper region of the two plots, where d_e is larger than d_i. One can recognise that the point distribution is slightly more compact in form I° compared to form II. This indicates that the packing in form I° is more efficient and that the structure contains fewer voids, which agrees well with the difference of 2% in the calculated densities of forms I° (D_c = 1.479 g cm^{-3}) and II (D_c = 1.449 g cm^{-3}). The analysis of Hirshfeld surfaces and 2D fingerprint plots provides further confirmation of our assessment that the molecules of the two polymorphs experience an almost identical environment. It also confirms that the differences in the packing modes, which lead to the doubling of the *c* axis in form I°, account for different properties of the polymorphs.

X-Ray powder diffractometry

A comparison of the published powder patterns of form II and the calculated pattern shows clearly that none of the form II samples reported in the literature[6,10] was pure but contaminated with form I. Fig. 8 shows an experimental powder pattern of a form II sample contaminated with form I° in comparison with the calculated powder patterns for the two pure phases. The experimental pattern was recorded at –100 °C to minimise temperature effects and increase the comparability with the pattern calculated from the low temperature single-crystal structures. The pattern of the mixture is representative for all diffractograms that have been designated as form II in the literature reports. Characteristic reflection positions, especially around 15–25° 2θ, show that each form contains unique reflections (form I°: 15.6, 17.7 and 22.2°; form II: 18.3 and 21.1°), which can be used to confirm the presence of either pure form I° or form II.

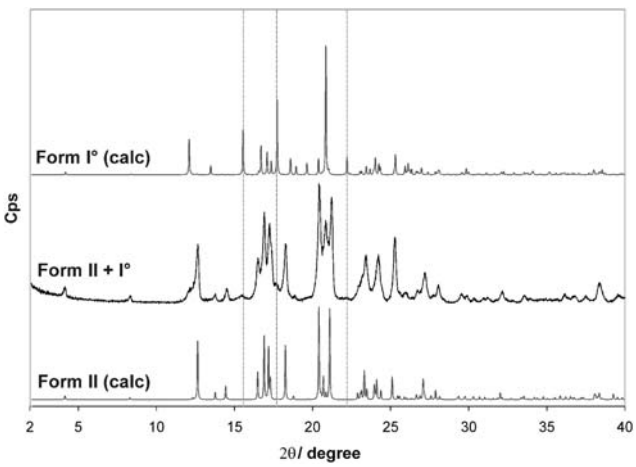

Fig. 8 Experimental (form II contaminated with form I°) *vs.* calculated (calc) powder patterns of aprepitant polymorphs (recorded at −100 °C). Characteristic reflections for form I° are highlighted with dotted lines.

Differential scanning calorimetry and thermodynamic stability

The two polymorphs of aprepitant were also examined by DSC measurements, which are given in Fig. 9. According to the patent literature, the two polymorphs show only weak differences in melting points and enthalpies of fusion.[6] The DSC curve of form I° exhibits a melting peak at 253.6 ± 0.1 °C (onset temperature) with an enthalpy of fusion of $\Delta_{fus}H_I$ = 53.7 ± 0.3 kJ mol^{-1}, whereas the melting point of form II is observed at 253.0 ± 0.1 °C ($\Delta_{fus}H_{II}$ = 52.4 ± 0.3 kJ mol^{-1}).

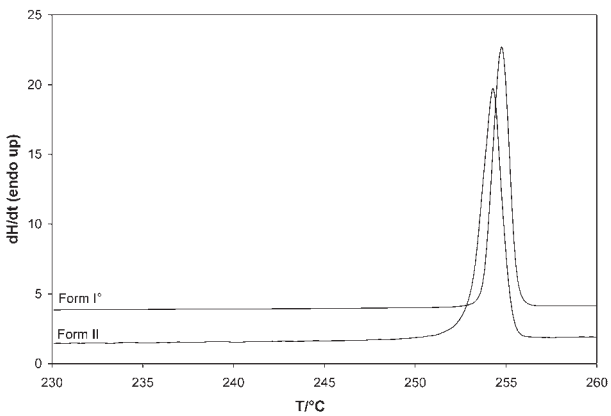

Fig. 9 DSC curves for aprepitant polymorphs (heating rate 10 K min^{-1}, open pan).

Since form I° melts at a higher temperature and exhibits a slightly higher enthalpy of fusion than modification II, we can conclude from the heat of fusion rule[31] that the two polymorphs are monotropically related. Form I° is thus the thermodynamically stable form in the entire temperature range. This was also verified by solution mediated transformation experiments, where a suspension of mixtures of the two forms in methanol or water was stirred at fluctuating temperatures (−10 to 50 °C). All experiments yielded pure form I° attesting that this is the thermodynamically stable modification in this temperature range. However, samples of form II, or mixtures of the two forms, stored at ambient conditions as well as under stress conditions (60 °C and 100% RH) did not transform to the stable modification I°, indicating the high kinetic stability of the metastable form II. A further confirmation of the fact that form I° is the thermodynamically stable form in the whole temperature range, can be derived from the order of densities I° > II. Since the forms differ mainly in the packing of identical molecular units, we can expect that the density rule[27] holds. Exceptions to this rule are mainly observed in pairs of polymorphs with conformationally distinct molecules in the asymmetric unit[32] or strong differences in hydrogen bonding.[33]

Conclusions

The two polymorphs of aprepitant represent a very interesting case of supramolecular aggregation. Though the molecule is characterised by six freely rotatable bonds, the molecular conformation is surprisingly similar in the two polymorphs. Thus we cannot classify this case as conformational polymorphism, which commonly terms the occurrence of multiple molecular conformations in different solid-state forms.[34] Since the structural difference is based on alternative packing arrangements of the same hydrogen-bonded domains, we may assign this case to packing polymorphism, which refers to a second subtype[13] of polymorphism that addresses distinct three-dimensional arrangements of equally shaped molecules through different molecular interactions. However, since this situation is common for totally rigid molecules or molecules with weak conformational flexibility, the aprepitant polymorphs represent in fact a rather exceptional case.

Moreover, the polymorphism of this substance also teaches us that the knowledge of the crystal structures of each polymorph can be of paramount importance in order to assess the purity of a certain phase. Only after a careful comparison of the calculated powder pattern with those stated in the literature[6,10] we were sure that form II was never obtained as a pure phase (as claimed) but always contained significant amounts of form I°. Before this finding we could neither recognise the purity of form II with infrared spectroscopy, where form II exhibits an additional band at 1140 cm^{-1}, nor with thermal analysis (DSC) because of the very small melting point difference of ~0.5 °C. However, the rather small differences in the melting temperatures and enthalpies of fusion are not surprising in view of the structural features of the two modifications. The minor structural differences may also explain the propensity of the two forms to crystallise concomitantly.[35]

Forms I and II exhibit a close 2D packing similarity, but a simple transformation mechanism between these modifications where their common 2D fragments are maintained and rotated by 90° against one another is obviously not feasible. Instead, a major reordering of the entire structure is required, which explains the high kinetic stability of the metastable form II. The situation is quite different in aspirin,[18] where the two stacking modes differ only by a simple translation of one 2D unit against the other. Subsequently, the metastable form II of aspirin transforms readily to form I.

This study highlights the fact that 2D packing relationships are a regular and important phenomenon in organic crystals which is intrinsically linked to polymorphism. It seems almost inevitable that crystal forms related in such a way will exhibit very similar physical properties, because both the molecular geometry and the spatial arrangements associated with most of the nearest-neighbour intermolecular interactions are almost perfectly preserved. This is the case, in particular, when packing polymorphism is based on a common multi-layer structure fragment of molecules, as in the case discussed here. Ultimate certainty about the presence of a packing similarity, its nature and degree can be gained by comprehensive comparison of the spatial arrangements in the different molecular environments (carried out by the XPac program[11] in this study). Techniques such as the comparison of geometric parameters associated with H-bonds and other specific intermolecular interactions and the analysis of Hirshfeld surfaces can reveal particular aspects which arise from such a relationship and can be very helpful tools for the detailed investigation of this phenomenon.

Acknowledgements

The authors would like to thank Sandoz GmbH for the financial support of this work. We further thank Ram K. R. Jetti for the help with the crystal structure refinement.

References

1 T. M. Dando and C. M. Perry, *Drugs*, 2004, **64**, 777–794.
2 J. Haleblian and W. Crone, *J. Pharm. Sci.*, 1969, **58**, 911–929; T. L. Threlfall, *Analyst*, 1995, **120**, 2435–2460.
3 H. G. Brittain and D. J. W. Grant, in *Polymorphism in Pharmaceutical Solids*, ed. H. G. Brittain, Marcel Dekker, New York, 1999, pp. 279–330; L. Yu, G. A. Stephenson, C. A. Mitchell, C. A. Bunnell, S. V. Snorek, J. J. Bowyer, T. B. Borchardt, J. G. Stowell and S. R. Byrn, *J. Am. Chem. Soc.*, 2000, **122**, 585–591; C. Sun and D. J. W. Grant, *Pharm. Res.*, 2001, **18**, 274–280; X. Chen, K. R. Morris, U. J. Griesser, S. R. Byrn and J. G. Stowell, *J. Am. Chem. Soc.*, 2002, **124**, 15012–15019.
4 J. Bernstein, *Polymorphism in Molecular Crystals*, Oxford University Press, Oxford, 2002, pp. 297–307.
5 Merck & Co., Inc., USA, WO 1995/16679 A1, 1995.
6 Merck & Co., Inc., USA, WO 1999/01444 A1, 1999.
7 J. J. Hale, S. G. Mills, M. MacCoss, P. E. Finke, M. A. Cascieri, S. Sadowski, E. Ber, G. G. Chicchi, M. Kurtz, J. Metzger, G. Eiermann, N. N. Tsou, F. D. Tattersall, N. M. J. Rupniak, A. R. Williams, W. Rycroft, R. Hargreaves and D. E. MacIntyre, *J. Med. Chem.*, 1998, **41**, 4607–4614.
8 Glenmark Pharmaceutical Limited, India, WO 2007/088483 A1, 2007.
9 Dr. Reddy's Laboratories Ltd., India, WO 2007/112457 A2, 2007.
10 R. Helmy, G. X. Zhou, Y. W. Chen, L. Crocker, T. Wang, R. M. Wenslow, Jr and A. Vailaya, *Anal. Chem.*, 2003, **75**, 605–611.

11 T. Gelbrich and M. B. Hursthouse, *CrystEngComm*, 2005, **7**, 324–336; Gelbrich and M. B. Hursthouse, *CrystEngComm*, 2006, **8**, 448–460.
12 J. J. McKinnon, M. A. Spackman and A. S. Mitchell, *Acta Crystallogr., Sect. B: Struct. Sci.*, 2004, **60**, 627–668; F. L. Hirshfeld, *Theor. Chim. Acta*, 1977, **44**, 129–138.
13 K. M. J. Brands, J. F. Payack, J. D. Rosen, T. D. Nelson, A. Candelario, M. A. Huffman, M. M. Zhao, J. Li, B. Craig, Z. J. Song, D. M. Tschaen, K. Hansen, P. N. Devine, P. J. Pye, K. Rossen, P. G. Dormer, R. A. Reamer, C. J. Welch, D. J. Mathre, N. N. Tsou, J. M. McNamara and P. J. Reider, *J. Am. Chem. Soc.*, 2003, **125**, 2129–2135; Y. Chen, G. X. Zhou, N. Brown, T. Wang and Z. Ge, *Anal. Chim. Acta*, 2003, **497**, 155–164; K. M. J. Brands, S. W. Krska, T. Rosner, K. M. Conrad, E. G. Corley, M. Kaba, R. D. Larsen, R. A. Reamer, Y. Sun and F.-R. Tsay, *Org. Process Res. Dev.*, 2006, **10**, 109–117; C. J. Cowden, R. D. Wilson, B. C. Bishop, I. F. Cottrell, A. J. Davies and U.-H. Dolling, *Tetrahedron Lett.*, 2000, **41**, 8661–8664.
14 L. J. Farrugia, *J. Appl. Crystallogr.*, 1999, **32**, 837–838; A. Altomare, M. C. Burla, M. Camalli, G. Cascarano, C. Giacovazzo, A. Guagliardi, A. G. G. Moliterni, G. Polidori and R. Spagna, *SIR97: a new program for solving and refining crystal structures*, Bari, Italy, 1997; G. M. Sheldrick, *Acta Crystallogr., Sect. A: Found. Crystallogr.*, 2008, **64**, 112–122.
15 Stoe & Cie GmbH, Darmstadt, 2006.
16 D. J. W. Grant, in *Polymorphism in Pharmaceutical Solids*, ed. H. G. Brittain, Marcel Dekker, New York, 1999, pp. 1–33.
17 M. C. Etter, *Acc. Chem. Res.*, 1990, **23**, 120–126.
18 G. L. Gartland and B. M. Craven, *Acta Crystallogr., Sect. B: Struct. Crystallogr. Cryst. Chem.*, 1974, **30**, 980–987.
19 All CSD (version 5.27) searches were performed using Conquest version 1.8 (Nov. 2005, 353518 entries) with the following filters used: 3D coordinates determined, not disordered, *R*-factor $<10\%$, no errors, not polymeric and only organics.
20 A. I. Kitaigorodskii, *Organic Chemical Crystallography*, Consultants Bureau, New York, 1961.
21 (*a*) A. D. Bond, R. Boese and G. R. Desiraju, *Angew. Chem., Int. Ed.*, 2007, **46**, 615–617; (*b*) A. D. Bond, R. Boese and G. R. Desiraju, *Angew. Chem., Int. Ed.*, 2007, **46**, 618–622.
22 T. Gelbrich, D. S. Hughes, M. B. Hursthouse and T. L. Threlfall, in preparation.
23 R. M. Vrcelj, J. N. Sherwood, A. R. Kennedy, H. G. Gallagher and T. Gelbrich, *Cryst. Growth Des.*, 2003, **3**, 1027–1032.
24 T. V. Timofeeva, V. N. Nesterov, F. M. Dolgushin, Y. V. Zubavichus, J. T. Goldshtein, D. M. Sammeth, R. D. Clark, B. Penn and M. Y. Antipin, *Cryst. Eng.*, 2000, **3**, 263–288; T. V. Timofeeva, V. N. Nesterov, R. D. Clark, B. Penn, D. Frazier and M. Y. Antipin, *THEOCHEM*, 2003, **647**, 181–202.
25 (*a*) A. Kálmán, L. Fábián, G. Argay, G. Bernáth and Z. Gyarmati, *J. Am. Chem. Soc.*, 2003, **125**, 34–35; (*b*) L. Fábián and A. Kálmán, *Acta Crystallogr., Sect. B: Struct. Sci.*, 2004, **60**, 547–558; (*c*) A. Kálmán, L. Fábián, G. Argay, G. Bernáth and Z. Gyarmati, *Acta Crystallogr., Sect. B: Struct. Sci.*, 2004, **60**, 755–762.
26 G. Desiraju and T. Steiner, *The Weak Hydrogen Bond (IUCr Monographs on Crystallography, No. 9)*, Oxford University Press, Oxford, 1999.
27 A. L. Spek, *J. Appl. Crystallogr.*, 2003, **36**, 7–13.
28 F. P. A. Fabbiani, D. R. Allan, S. Parsons and C. R. Pulham, *Acta Crystallogr., Sect. B: Struct. Sci.*, 2006, **62**, 826–842; P. Lozano-Casal, D. R. Allan and S. Parsone, *Acta Crystallogr., Sect. B: Struct. Sci.*, 2005, **61**, 717–723; J. J. McKinnon, F. P. A. Fabbiani and M. A. Spackman, *Cryst. Growth Des.*, 2007, **7**, 755–769; S. A. Moggach, D. R. Allan, S. Parsons and L. Sawyer, *Acta Crystallogr., Sect. B: Struct. Sci.*, 2006, **62**, 310–320; P. Munshi, B. W. Skelton, J. J. McKinnon and M. A. Spackman, *CrystEngComm*, 2008, **10**, 197–206.
29 S. K. Wolff, D. Grimwood, J. McKinnon, D. Jayatilaka and M. Spackman, *Crystal Explorer, Version 2.0*, University of Western Australia, Perth, 2007, (http://www.hirshfeldsurface.net/CrystalExplorer/).
30 M. A. Spackman and J. J. McKinnon, *CrystEngComm*, 2008, **4**, 378–392.
31 A. Burger and R. Ramberger, *Microchim. Acta*, 1979, **2** 273–316; A. Burger and R. Ramberger, *Microchim. Acta*, 1979, **2**, 259–271; L. Yu, *J. Pharm. Sci.*, 1995, **84**, 966–974.
32 U. J. Griesser, R. Jetti, M. F. Haddow, T. Brehmer and R. K. Harris, *Cryst. Growth Des.*, 2008, **8**, 44–56; X. Chen, K. R. Morris, U. J. Griesser, S. R. Byrn and J. G. Stowell, *J. Am. Chem. Soc.*, 2002, **124**, 15012–15019; J. Bauer, S. Spanton, R. Henry, J. Quick, W. Dziki, W. Porter and K. Morris, *Pharm. Res.*, 2001, **18**, 859–866.
33 U. J. Griesser, A. Burger and K. Mereiter, *J. Pharm. Sci.*, 1997, **86**, 352–358; S. M. Sharma, V. Vijayakumar, S. K. Sikka and R. Chidambaram, *Pramana*, 1985, **25**(1), 75–79.
34 J. Bernstein and A. T. Hagler, *J. Am. Chem. Soc.*, 1978, **100**, 673–681; J. Bernstein, Conformational Polymorphism, in *Organic Solid State Chemistry*, ed. G. R. Desiraju, Elsevier, Amsterdam, 1987, pp. 471–518; J. Bernstein, *Polymorphism in Molecular Crystals*, Clarendon Press, Oxford, 2002.
35 J. Bernstein, R. J. Davey and J.-O. Henck, *Angew. Chem., Int. Ed.*, 1999, **38**, 3441–3461.